LECTURE 7

SELECTED TOPICS IN THE LOW-SPEED AERODYNAMICS

The sources of a graphical material used in this lecture are:

[UA] D. McLean, Understanding Aerodynamics. Arguing from the Real Physics. Wiley, 2013.
[AES] Houghton E.L. et al., Aerodynamics for Engineering Students. 6th Ed. Elsevier, 2013.
[FVA] Drela M., Flight Vehicle Aerodynamics. MIT Press, 2014.

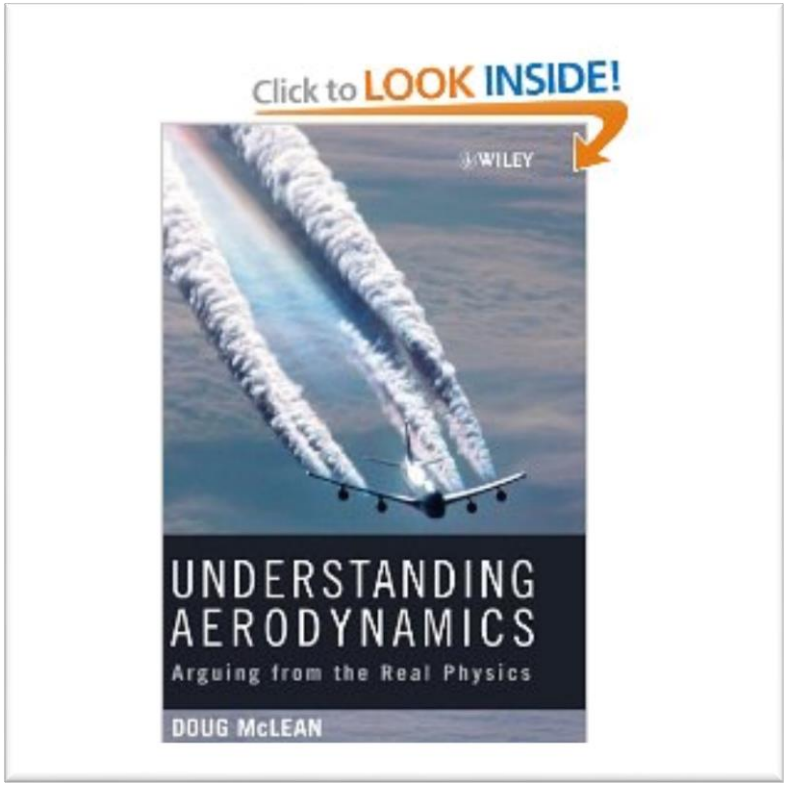

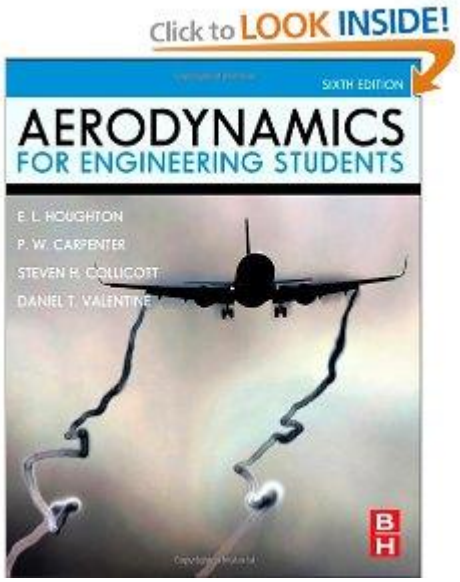

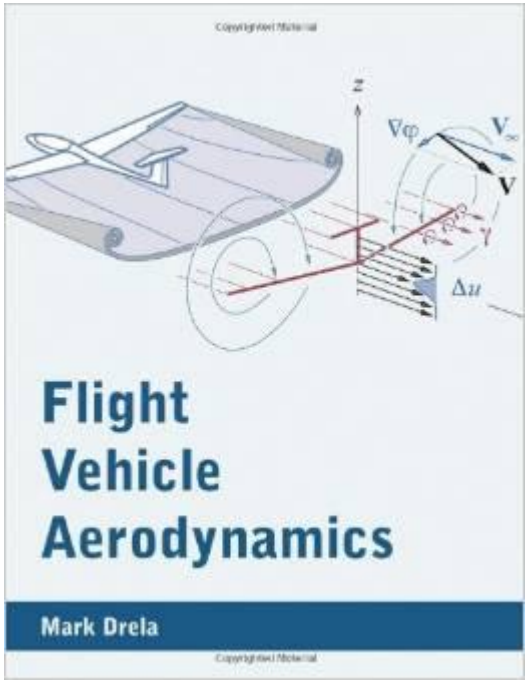

Problems to be addressed …

1. Thin-airfoil theory revisited – comparison to more sophisticated models.

2. Laminar airfoils, low-Reynolds number flow phenomena.

3. Flow pas multi-element airfoils

4. Flows past bluff (i.e., not streamlined) bodies

Thin airfoil theory -revisited

Accordingly to **linear** TAT, three factors influencing the aerodynamic properties oh a thin airfoil: angle of attach, camber and thickness can be analyzed separately. The total effect is just a superposition of these factors.

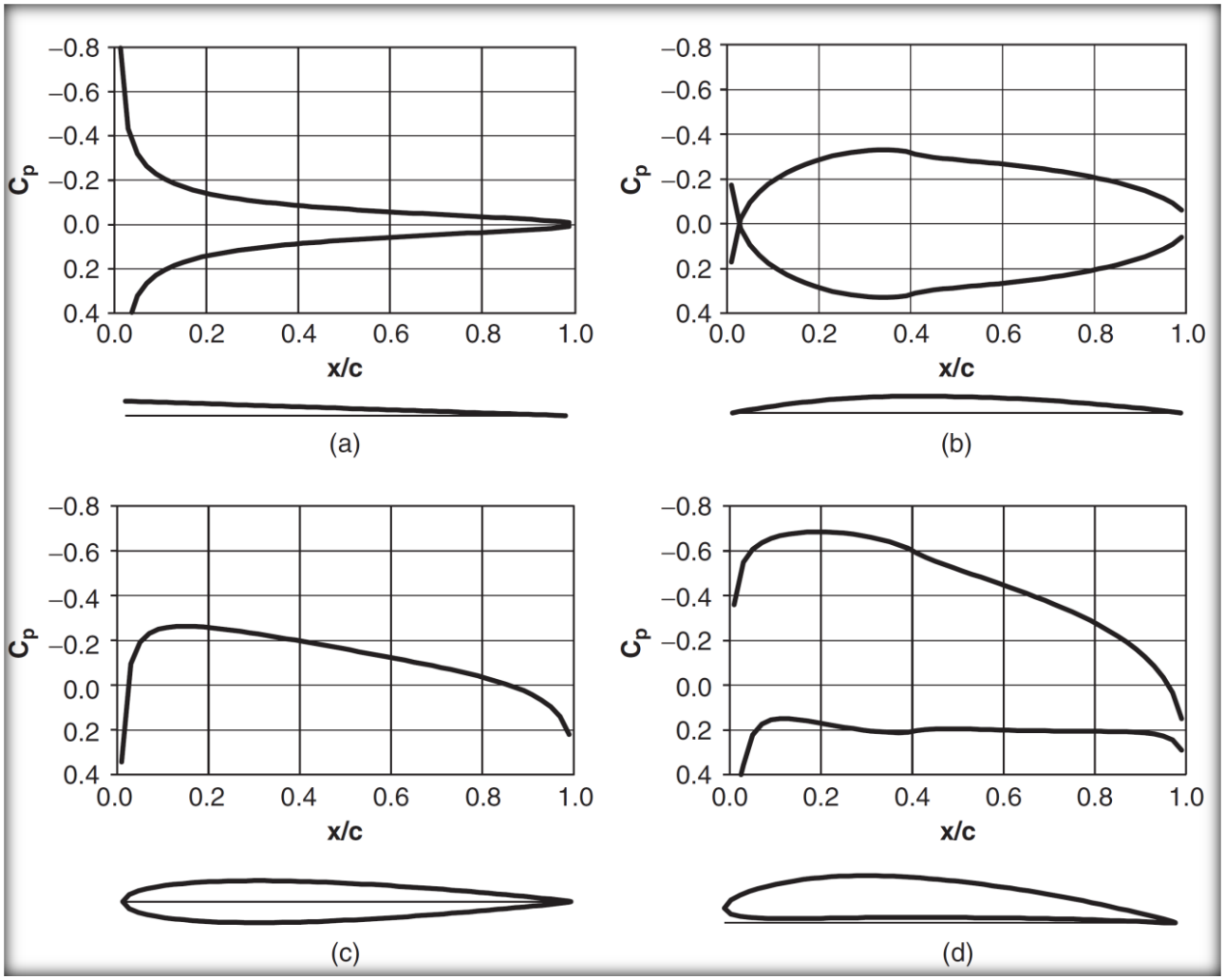

Pressure coefficient

$$C_p = \frac{p - p_\infty}{q_\infty} \quad , \quad q_\infty = \tfrac{1}{2}\rho V_\infty^2$$

for:

a) Flat plate, AoA is $\alpha = 2^0$

b) Camber line, $\alpha = 0^0$ (as for the NACA 44** airfoils)

c) Symmetric airfoils with 10% thickness (NACA **10), $\alpha = 0^0$

d) Effect of superposition: NACA 4410, $\alpha = 2^0$

TAT vs full potential calculations (program MSES)

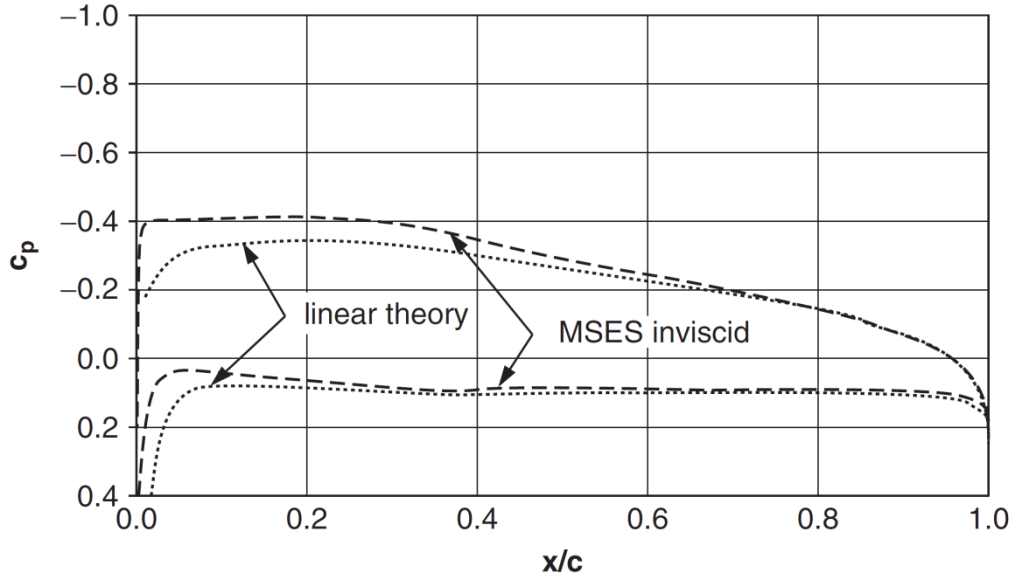

NACA 2405, $\alpha = 1^0$

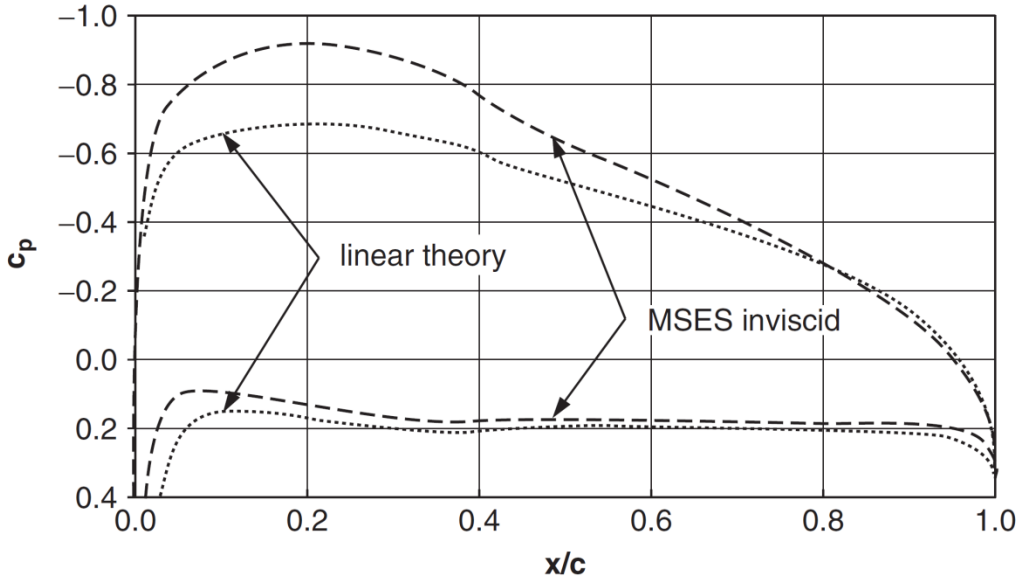

NACA 4410, $\alpha = 2^0$

Visscous effect (the presence of the boundary layer)

External potential flow is shaped differently because of the displacement effect. Related is a modified pressure distribution which violates the d'Alembert paradox – now the **pressure component of the aerodynamic drag appears!**

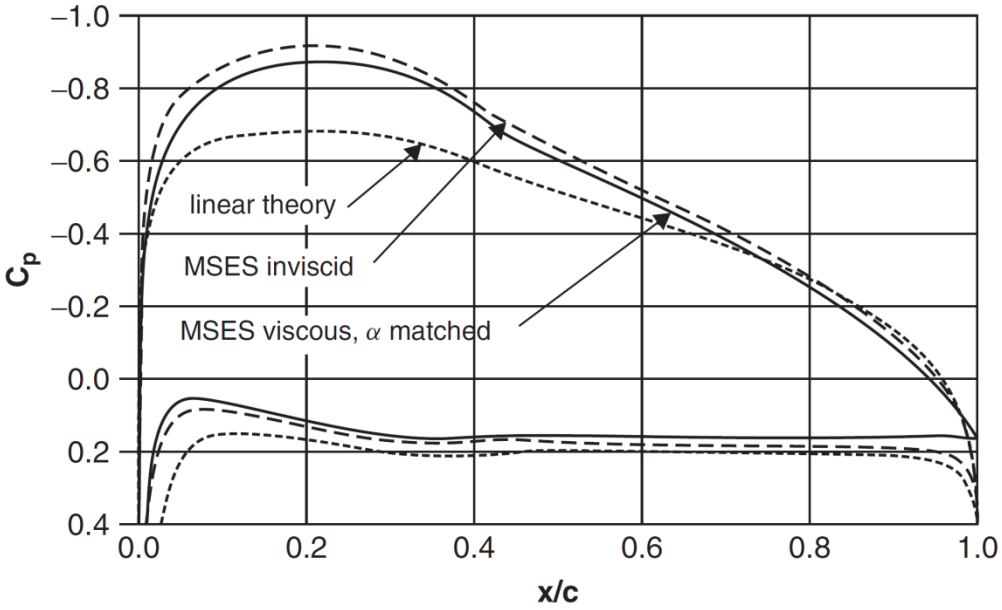

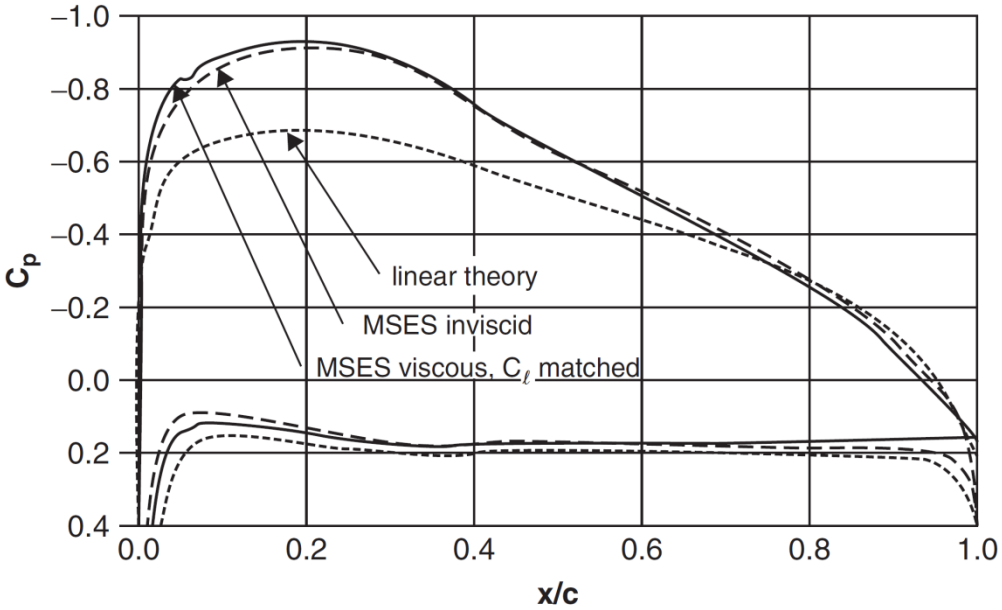

Comparison of the pressure distributions at the NACA 4410 airfoil computed with: linear theory, full potential solution (MSES inviscid) and the hybrid method which account for the BL (MSES viscous). Re = 10 mln, the laminar turbulent transition forces at the distance of 5% chord form. AoA: left $\alpha_{linear} = \alpha_{potential} = \alpha_{BL} = 2^o$**, right** $\alpha_{linear} = \alpha_{potential} = 2^o$, $\alpha_{viscous} = 2.54^o$ **(such that** $C_L = 0.739$ **in both cases).**

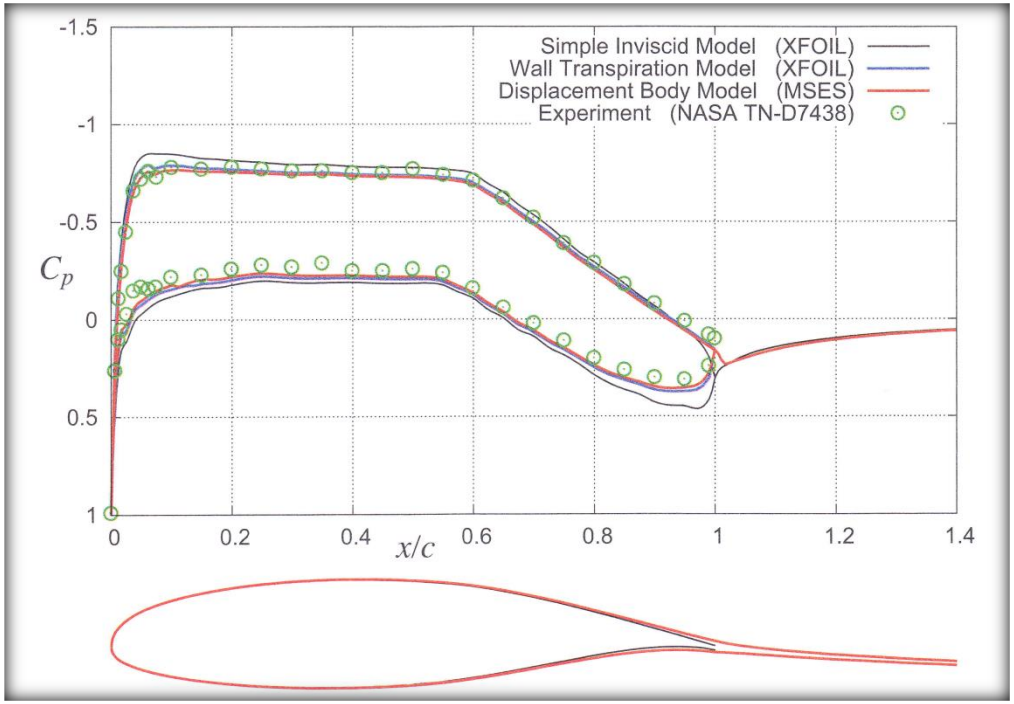

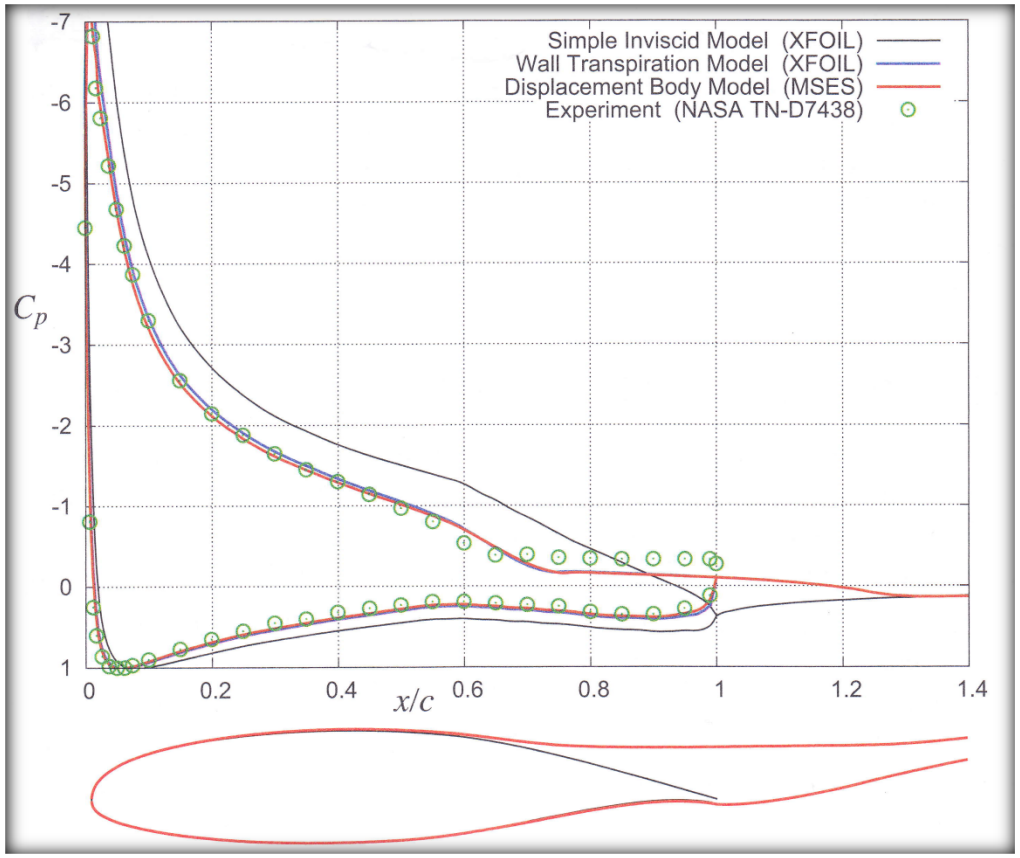

Laminar airfoil GAW(1), Re = 6 mln.

Left: AoA is $\alpha = 0^0$. The contour of a „displacement body" (DB) is shown in red. BL is thin and fully attached, hence the DB contour nearly overlaps with the physical contour.

Right: AoA is $\alpha = 16^0$. This time – due to the BL separation - the shape of the DB is significantly different that the physical body.

Good agreement of MSES and XFOIL predictions with experimental findings is visible.

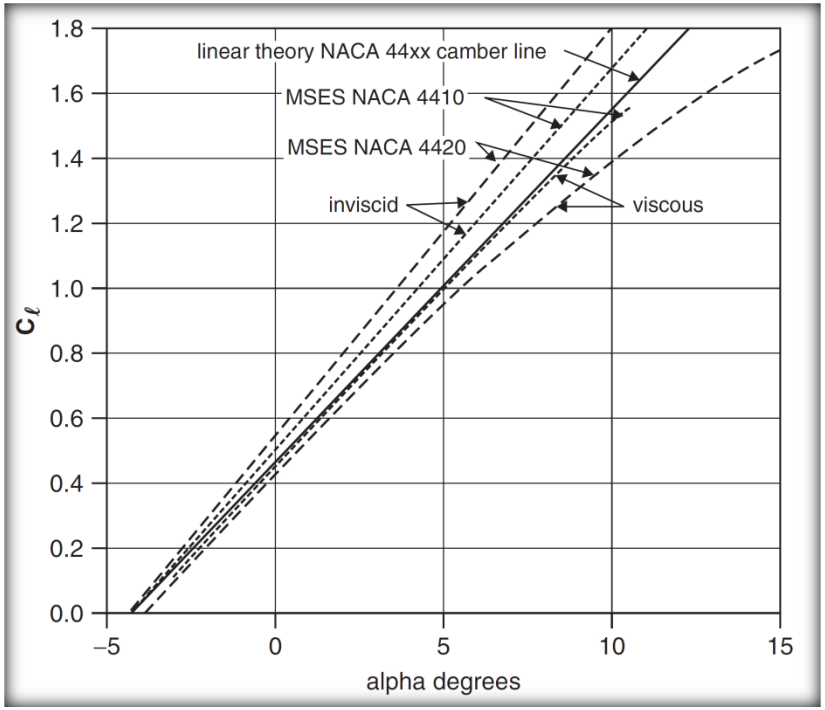

Lift characteristics of NACA 4410 (10% thickness) and NACA 4420 (20% thickness) obtained from linear theory, full potential theory without and with boundary layer effects (program MSES by M. Drela, MIT).

The "fatness paradox" is visible: the slope of the "inviscid" case increases with the thickness, but the slope of the "viscous" (thus, realistic) case – decreases.

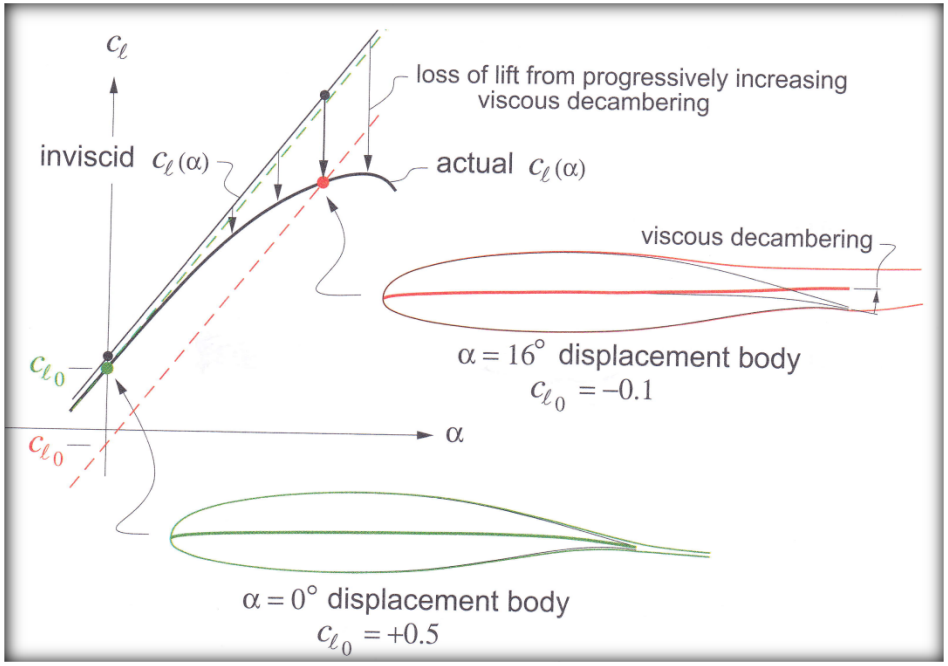

Effect of „viscous decambering": the apparent camber line of the "displacement body" seems to have less curvature than real, geometric camber. The actual camber can even have the opposite sign and works as a flap at slightly negative angle (so called "viscous flap")/

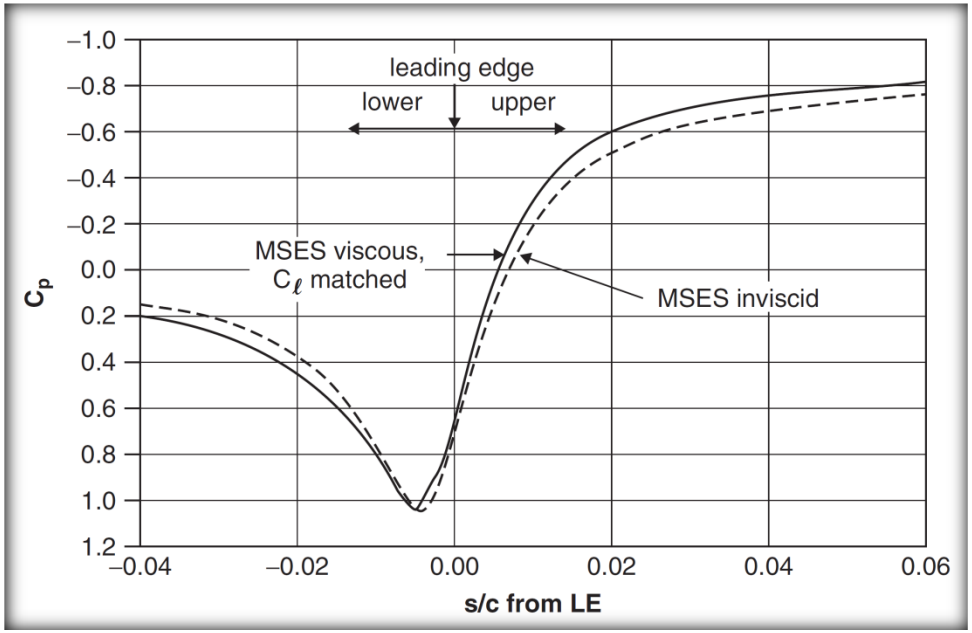

Pressure distribution near the front stagnation point in the inviscid and viscous (C_L- matched) calculation with the MSES program. The AoA is $\alpha = 2^0$ for inviscid case and $\alpha = 2.54^0$ for viscous case. The Reynolds number is Re = 10 mln.

Clearly, the viscosity effect are pretty weak in this region.

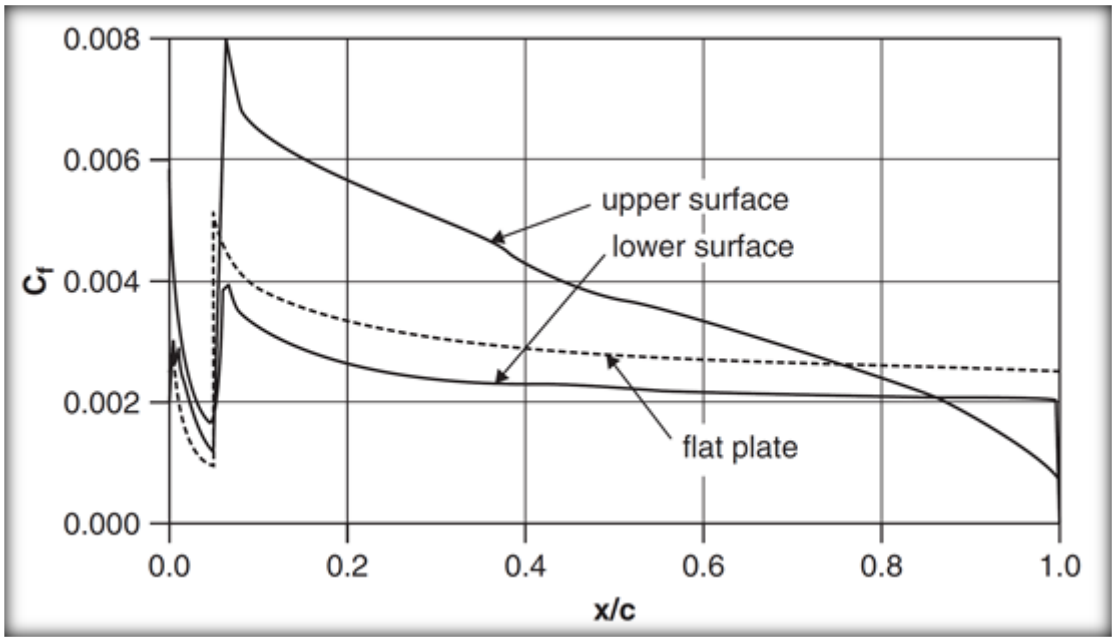

Distribution of the skin friction coefficient at NACA 4410. AoA is $\alpha = 2.54^0$, the Reynolds number Re = 10^7, the LT transition is forces at the distance of 5% chord from the LE.

For comparison sake, the distribution of skin friction coefficient along the flat plate at zero AoA is shown (dashed line).

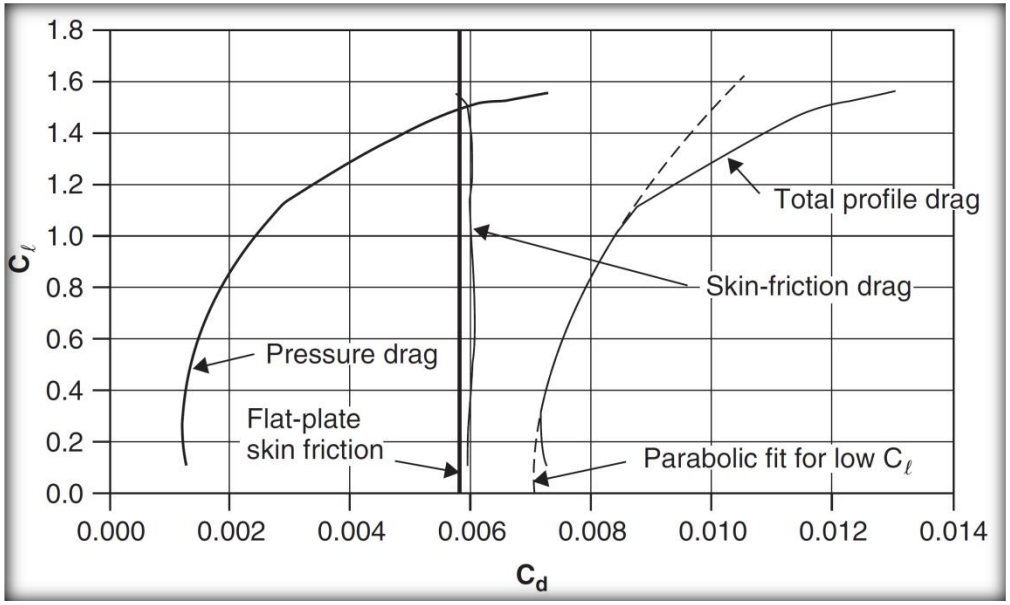

Division of the aerodynamic drag into skin-friction and pressure components shown for the NACA 4410 airfoil. The flow parameter as before.

It can be seen that for a small AoA the pressure component constitutes over a dozen percent of the total drag. In the range of linear C_L-vs-AoA dependence, the pressure drag coefficient increases with the square of the lift coefficient, but beyond this range – much faster.

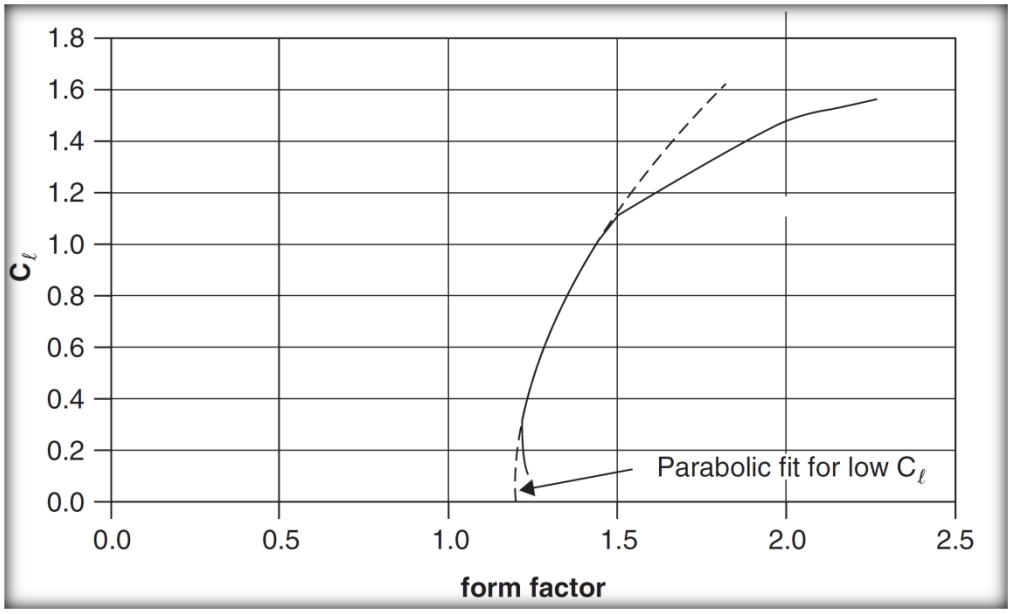

The form factor is defined as the ratio of the total airfoil to the skin-friction drag of the flap plate in the same flow conditions.
In the left – the drag polar for NACA 4410 plotted in terms of lift-coefficient and the form factor.

Laminar airfoils – general information

Idea: To shape an airfoil in such a way that the area of nearly-zero pressure gradient appears on the suction side, which will keep the boundary layer laminar and attached along relatively long distance. Then, the pressure recovery region should be design to trigger the LT transition before laminar separation occurs and such that emerging turbulent BL entails small drag penalty.

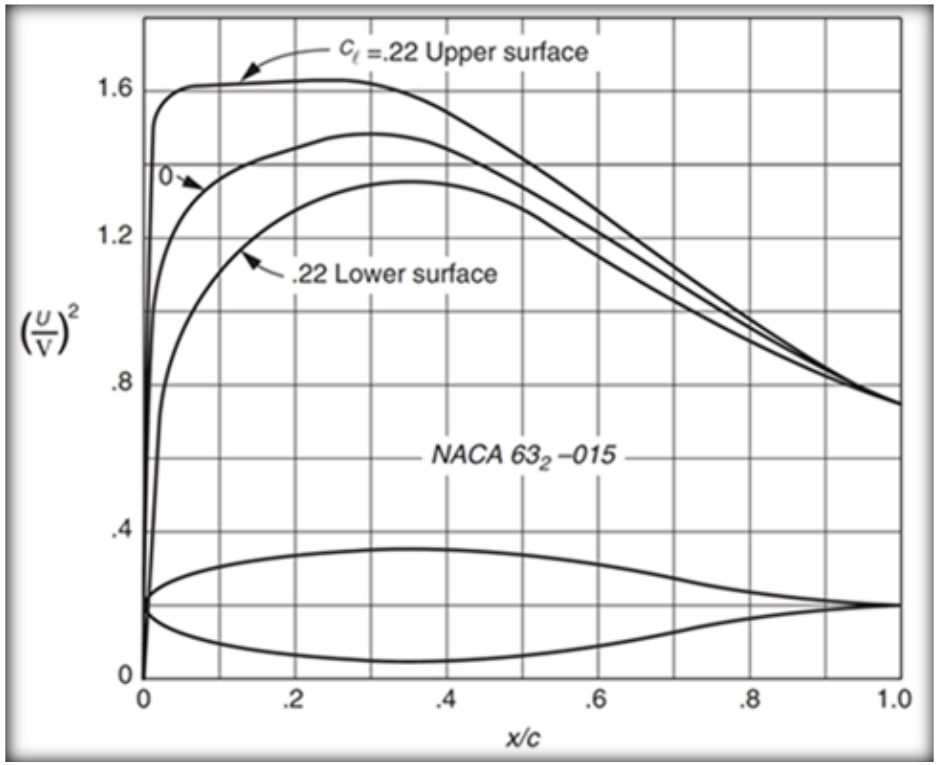

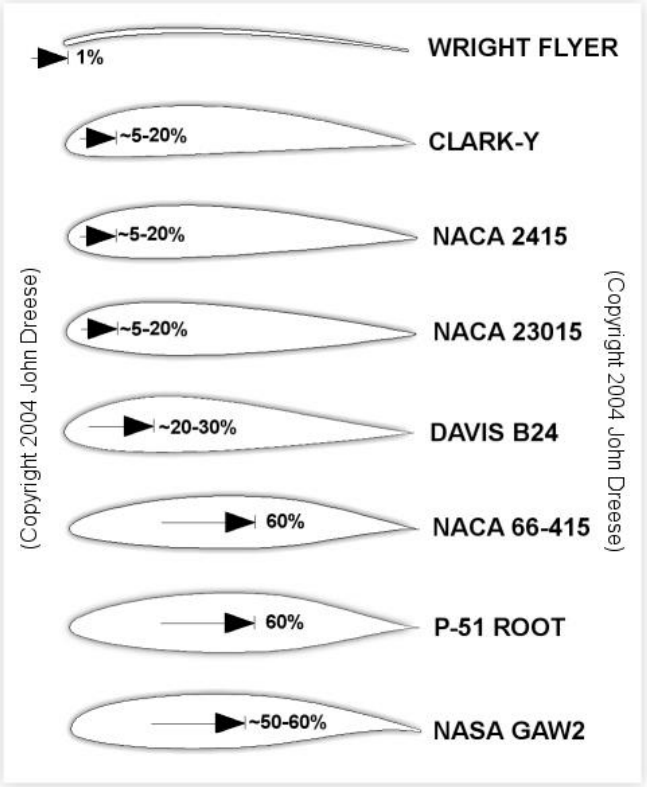

FIGURE 2: Extent of laminar flow on some famous airfoils.

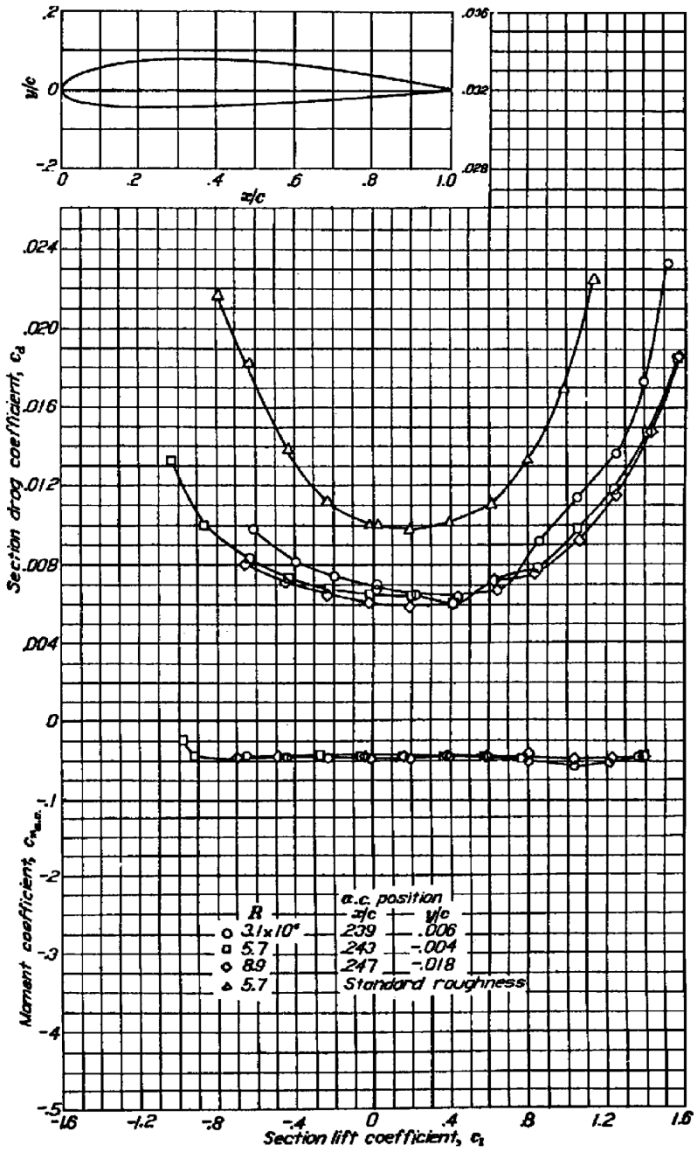

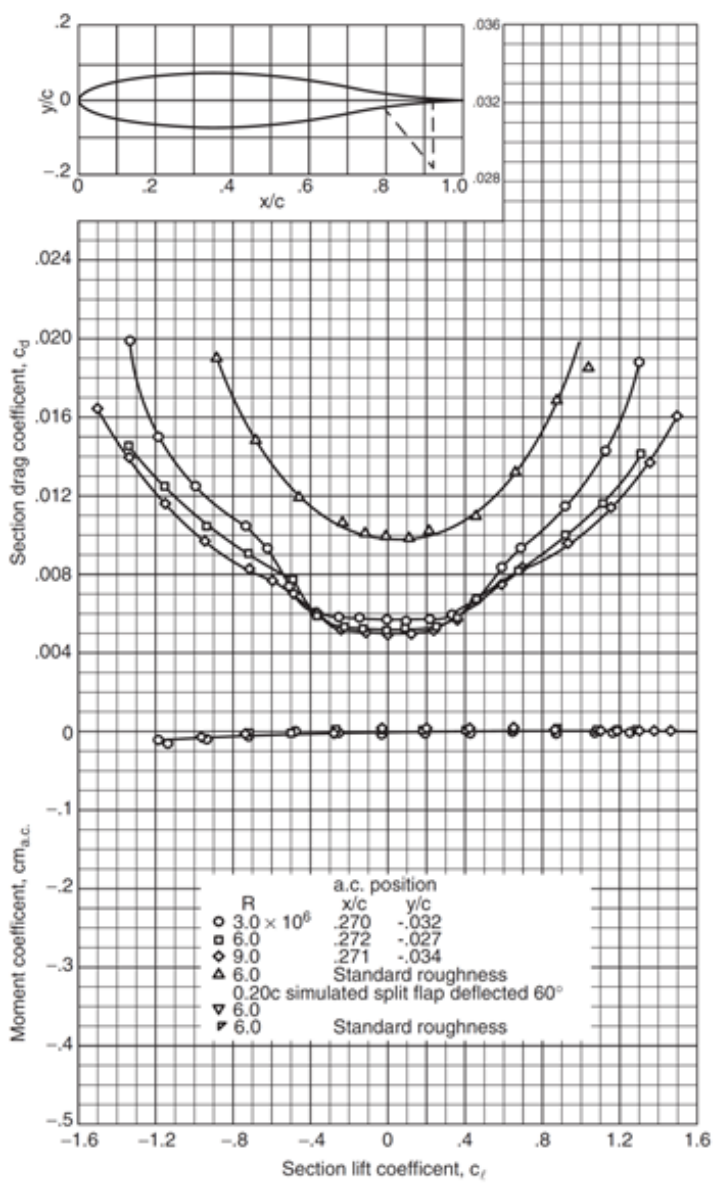

Drag polar of an "ordinary" (left) and the laminar airfoil NACA 63_2-015 (right). The characteristic "laminar bucket" can be noticed for the laminar airfoil. Another example on the next page …

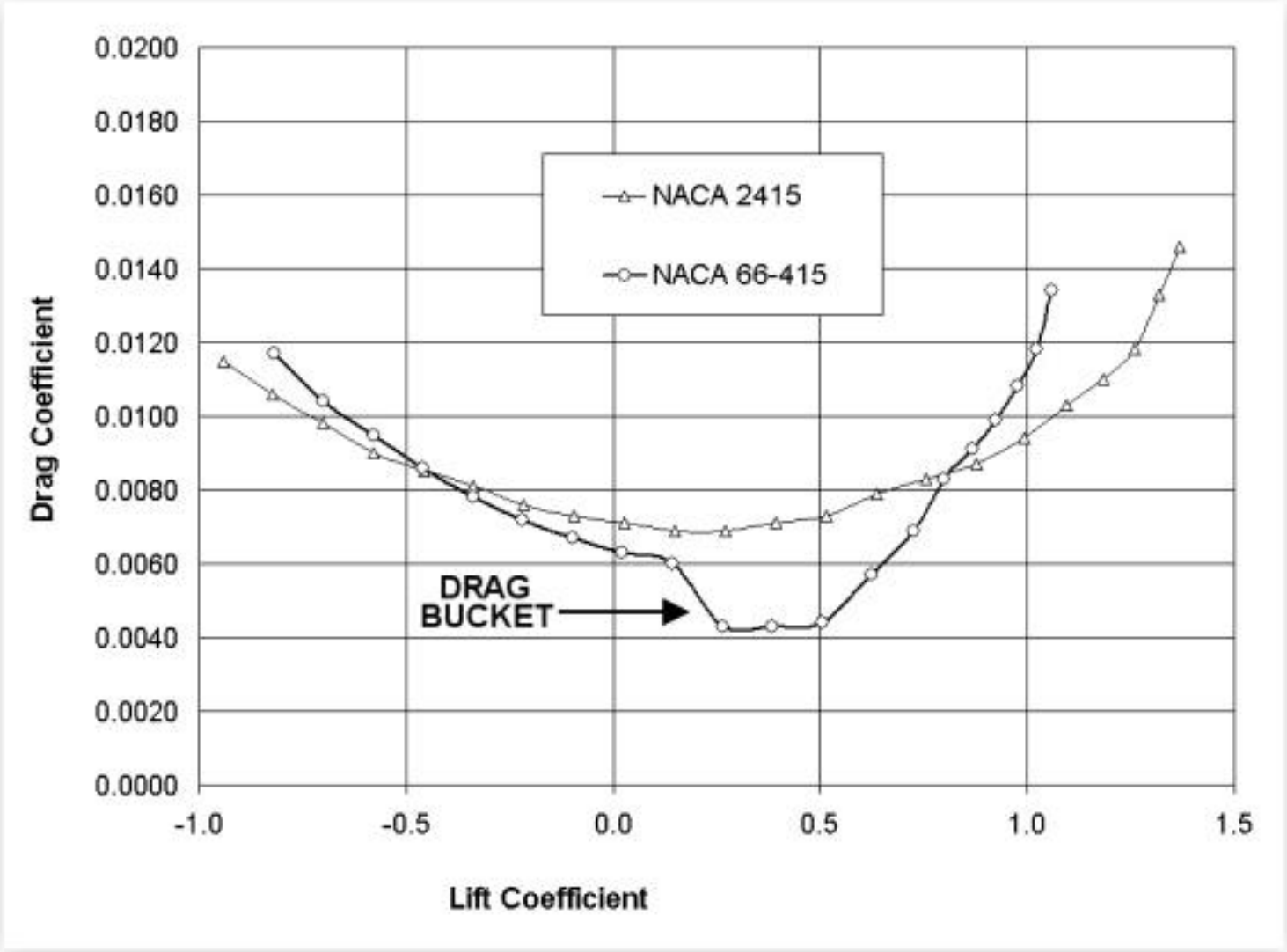

FIGURE 3: Laminar airfoil and non-laminar airfoil drag polar chart comparisons.

Key issue – **avoid at any cost a massive laminar separation**! Such separation leads to a very abrupt stall (sudden drop of the lift accompanied by an immense increase of drag). Typical remedy – **destabilize the laminar BL before it separates**.

The point is to choose right length of the laminar part and shape the pressure recovery region so that the turbulent BL does not separate but its friction drag is law. It turn out that a proper shape of a pressure recovery is concave, i.e., corresponding value of the second derivative of the pressure distribution is negative. It means that the positive pressure gradient should decrease while approaching the trailing edge. Refer to the section 9.2 in AES and the section 7.4.3 in UA for details.

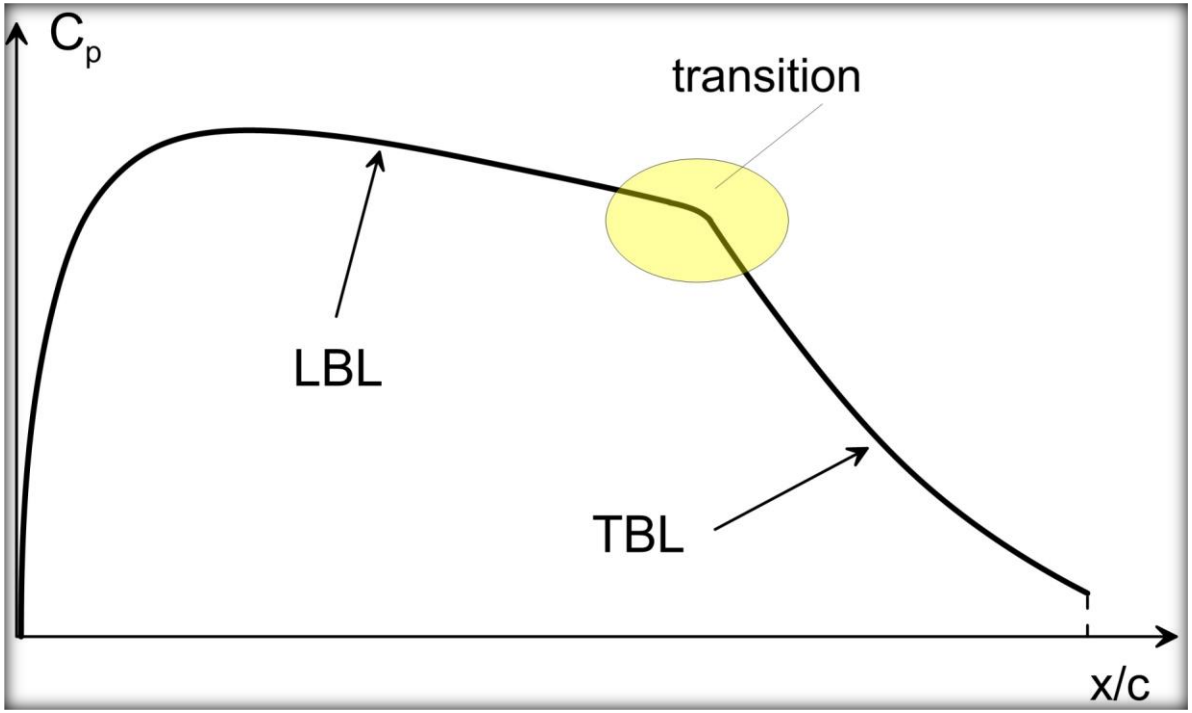

Conceptual plot of the pressure distribution along the suction side of a laminar airfoil in the "design" conditions.

Flow with a bounded laminar separation (a laminar bubble)

In the flow with lower Reynolds numbers (say, $\mathrm{Re} \simeq 10^5 \div 10^6$), a laminar boundary layer has a tendency to separate. The reversed flow in the separation region is strongly unstable and may undergo transition to turbulence and then re-attach to the wall. If so, the closed laminar region appear called a laminar bubble. The BL behind the bubble is turbulent, however, its thickness is large and, hence, its resistivity to further separation is limited. Therefore, the location of the bubble and the value of pressure to be "recovered" behind the bubble is essential.

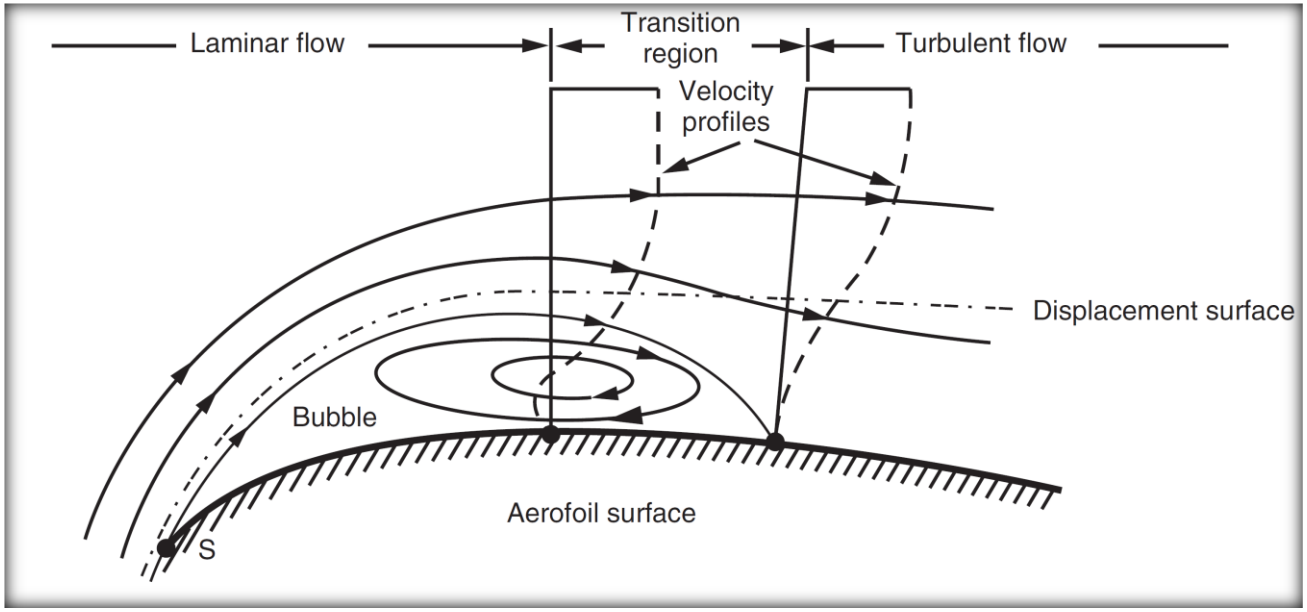

General structure of the separation bubble

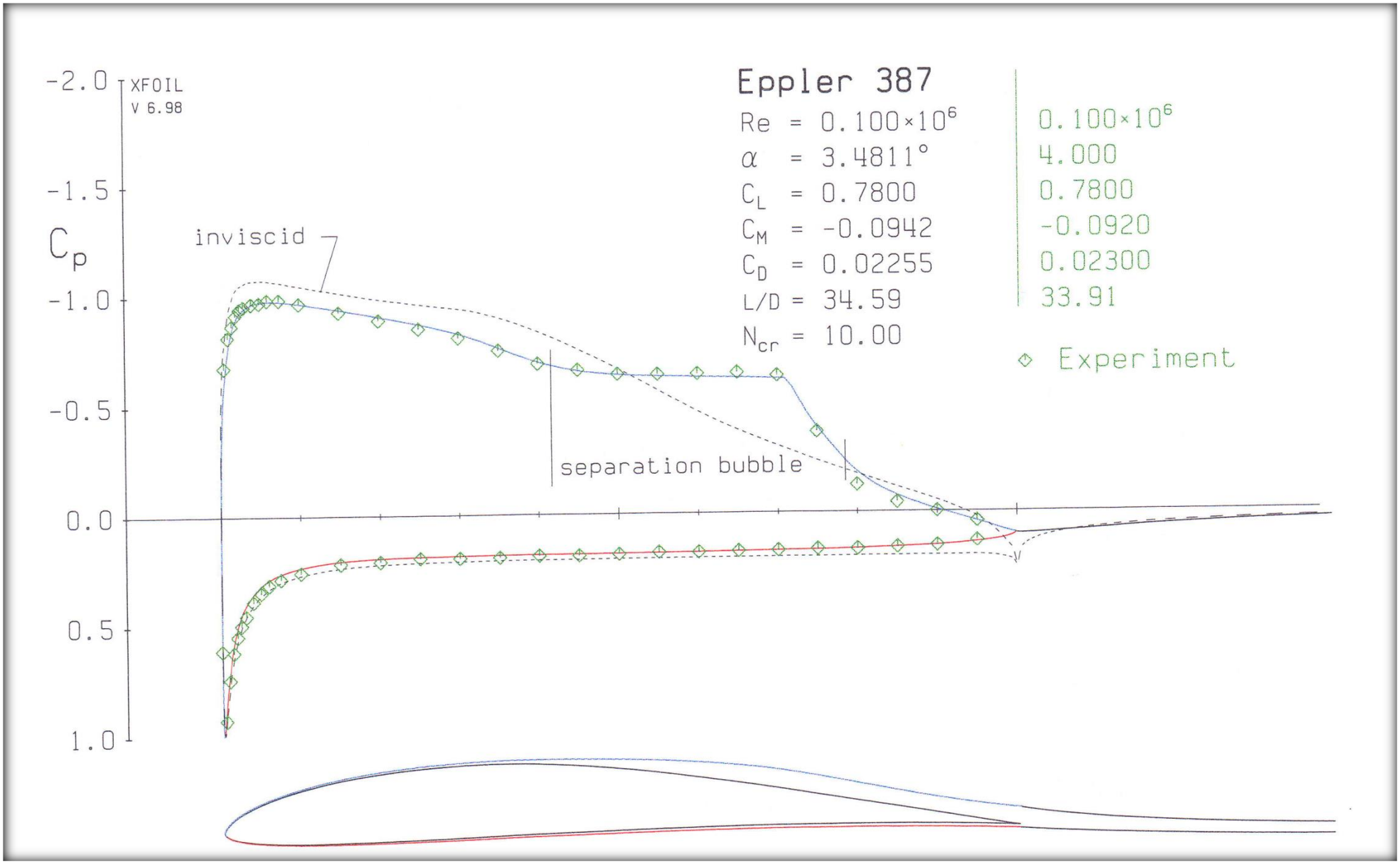

Low-Reynolds number flow past the Epler 387 airfoil with huge laminar bubble.

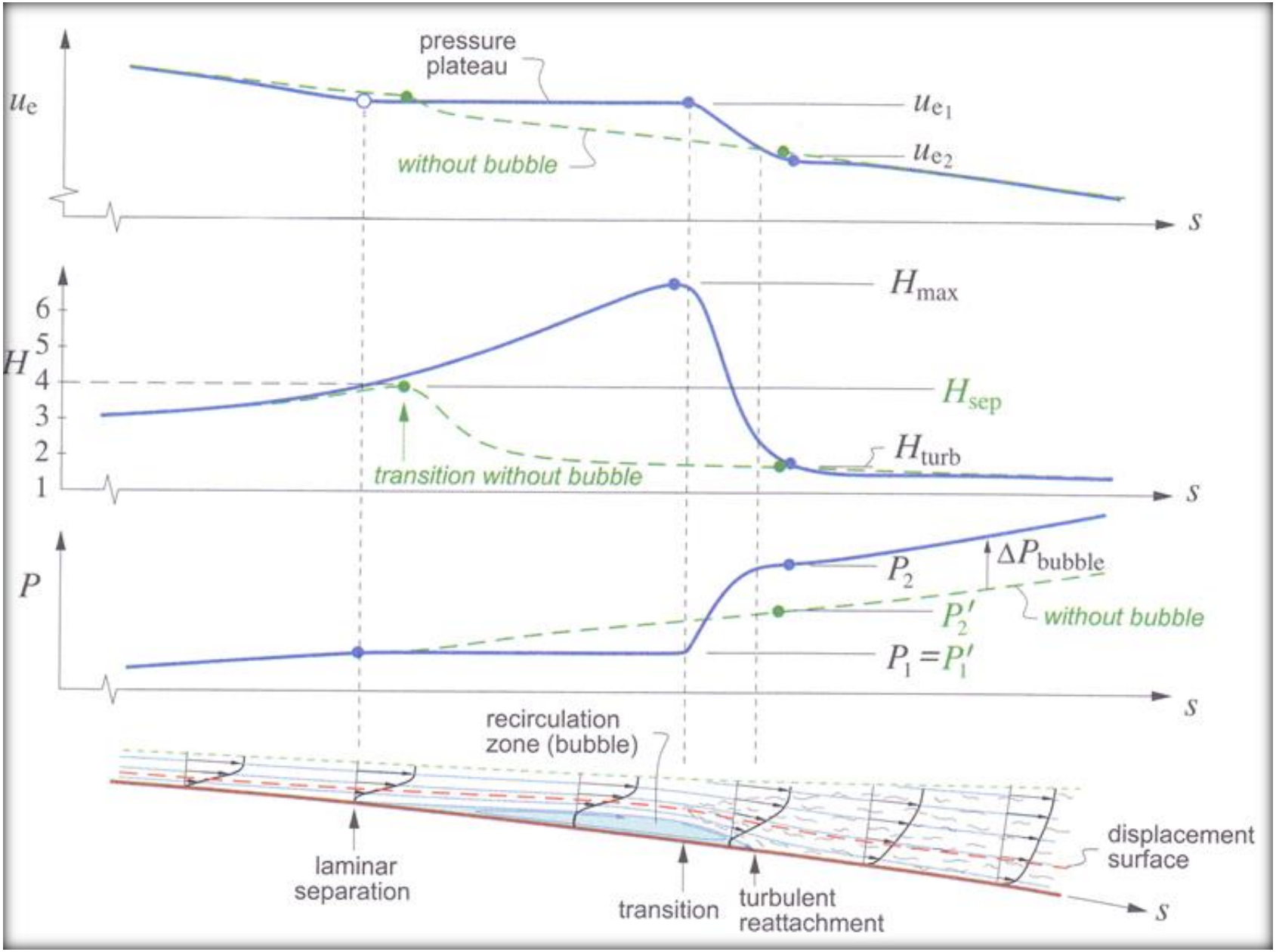

Structure of the flow inside the separation bubble at the Epler 387.

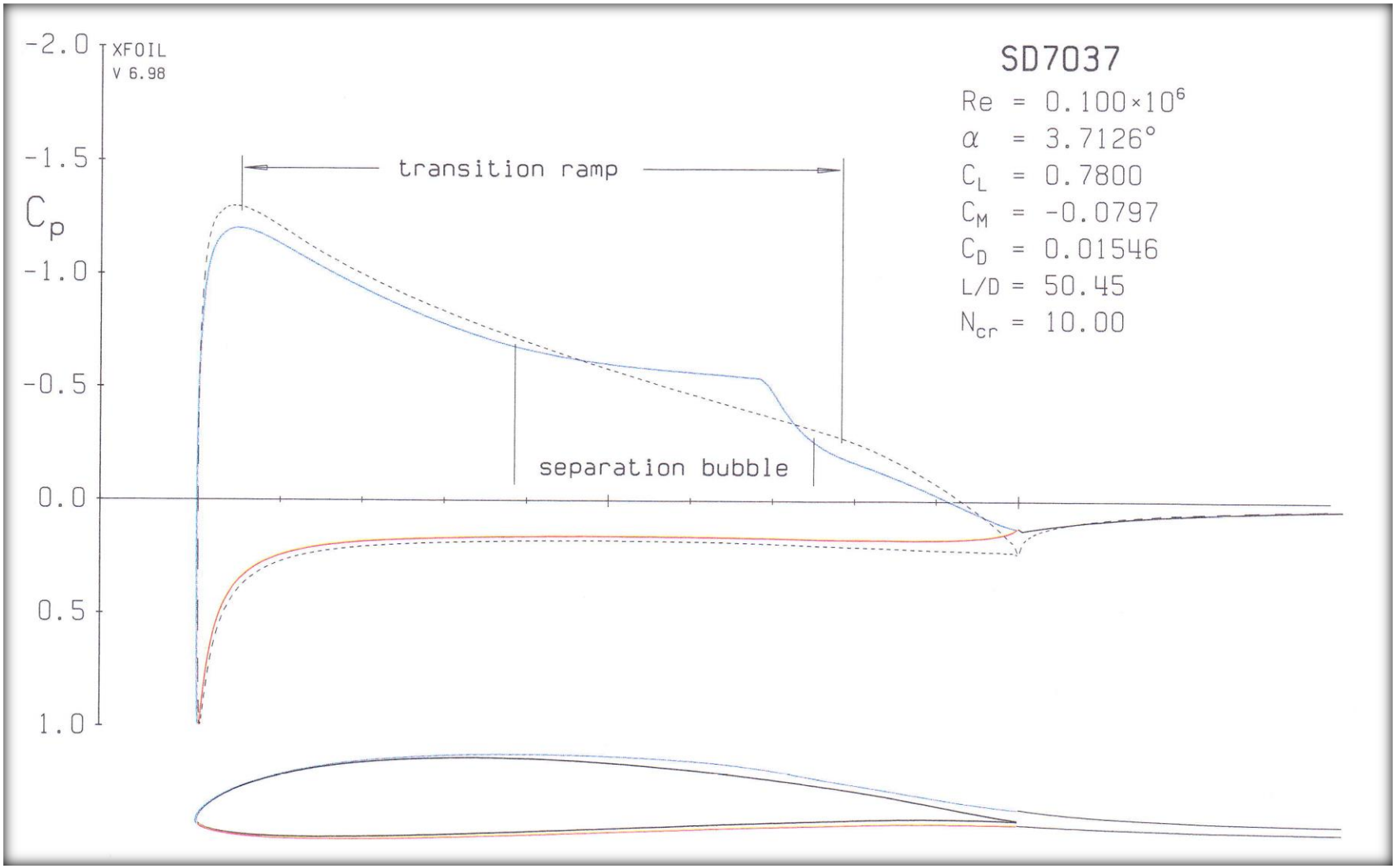

Airfoil design which properly accounts for the presence of the separation bubble. In the condition of the same Reynolds number the airfoil SD7037 achieves the same lift force as Epler 387 with the drag penalty smaller by nearly 1/3!

Flow past multi-element wing sections

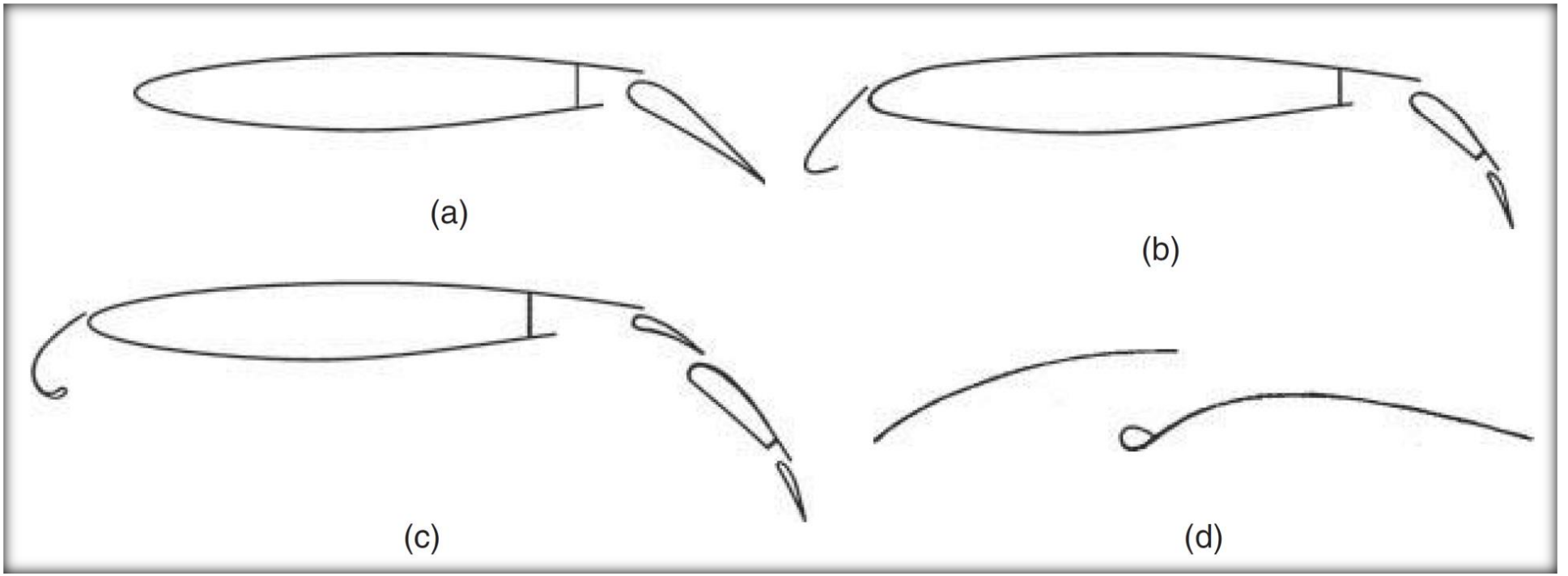

(a) simple flap, (b) slat and two-element rear flap (Boeing 757, 737 NG), (c) front elastic Krueger slat and triple-element rear flap (Boeing 747), (d) jib-mainsail rig of a sailing boat.

Aerodynamic interaction in a multi-element wing section

1. A boundary layer at each element should start from the “fresh stream” and hence its thin and less prone for transition and separation.

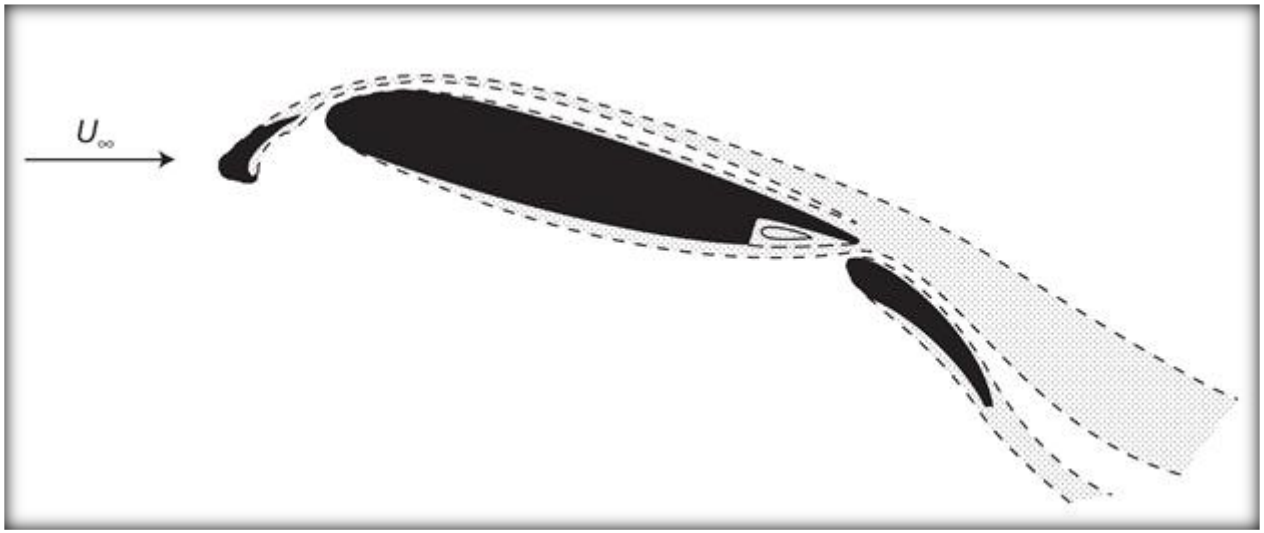

2. Slat’s (front flap) role is mostly to change the direction of the local flow direction in the vicinity of the leading edge of the main elements. In effect, the suction pressure in the front part of the main element is reduced (this element gets “unloaded”). Consequently, the average gradient needed for pressure recovery on the main element is smaller which facilitates the flow without boundary layer separation.

3. Rear flap causes the flow near the main element trailing edge to be faster and with lower pressure. This farther reduces pressure recovery gradient on the main element.

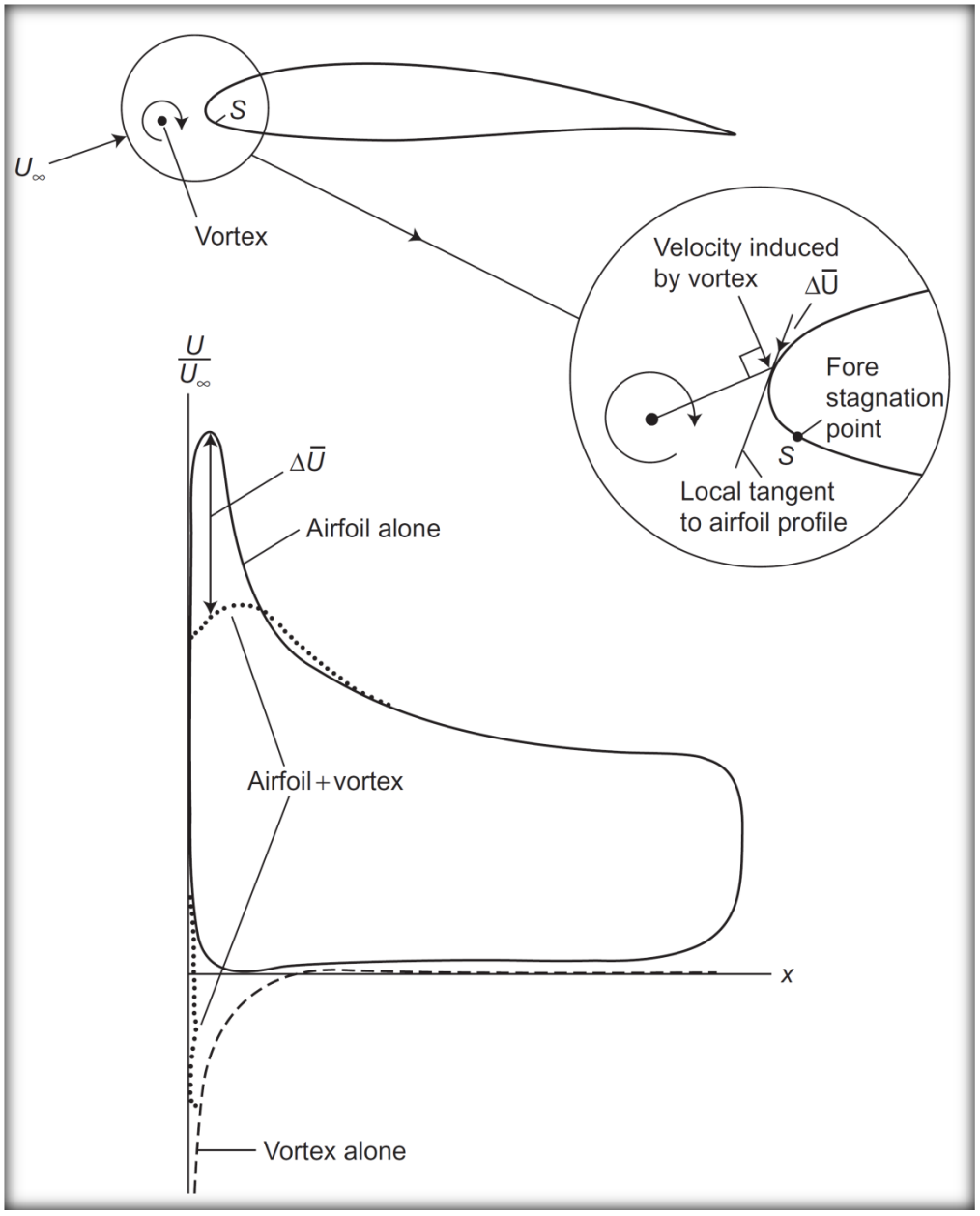

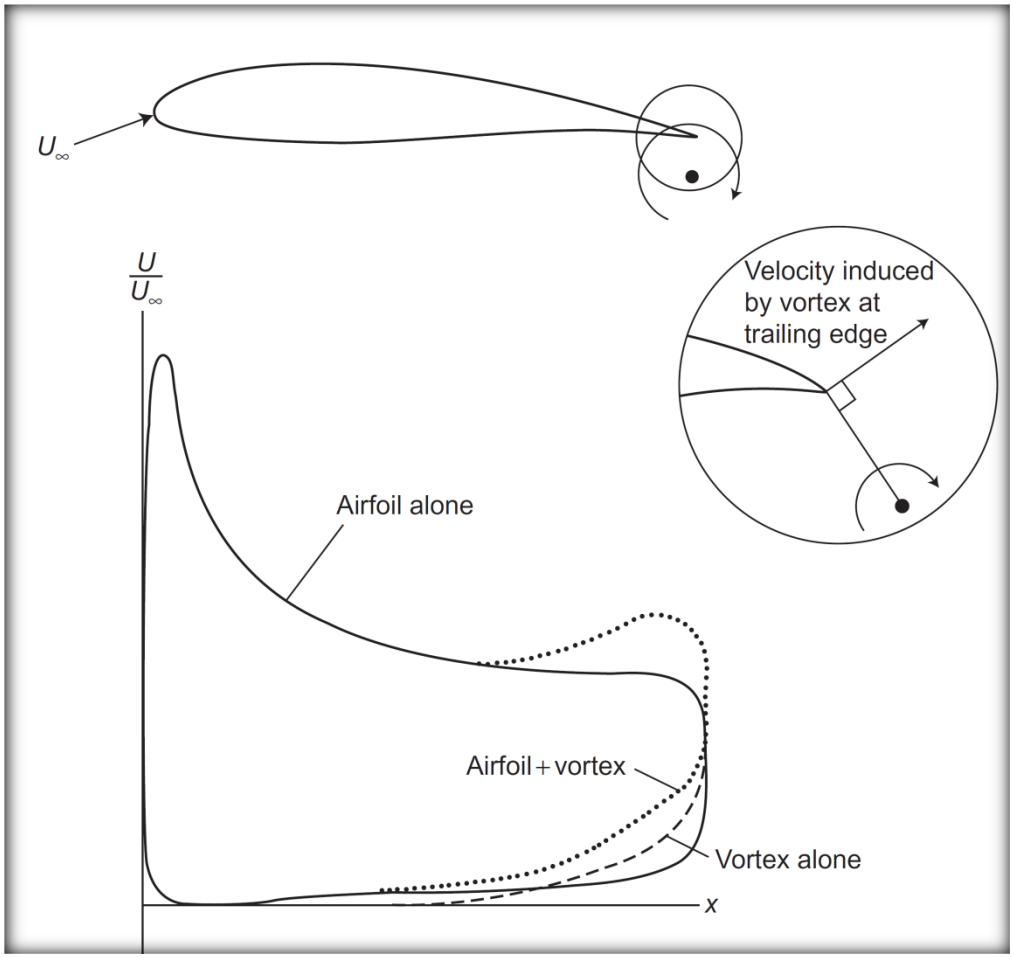

Action of a slat and a rear flap explained by means of the simple point vortex (lumped circulation) model.

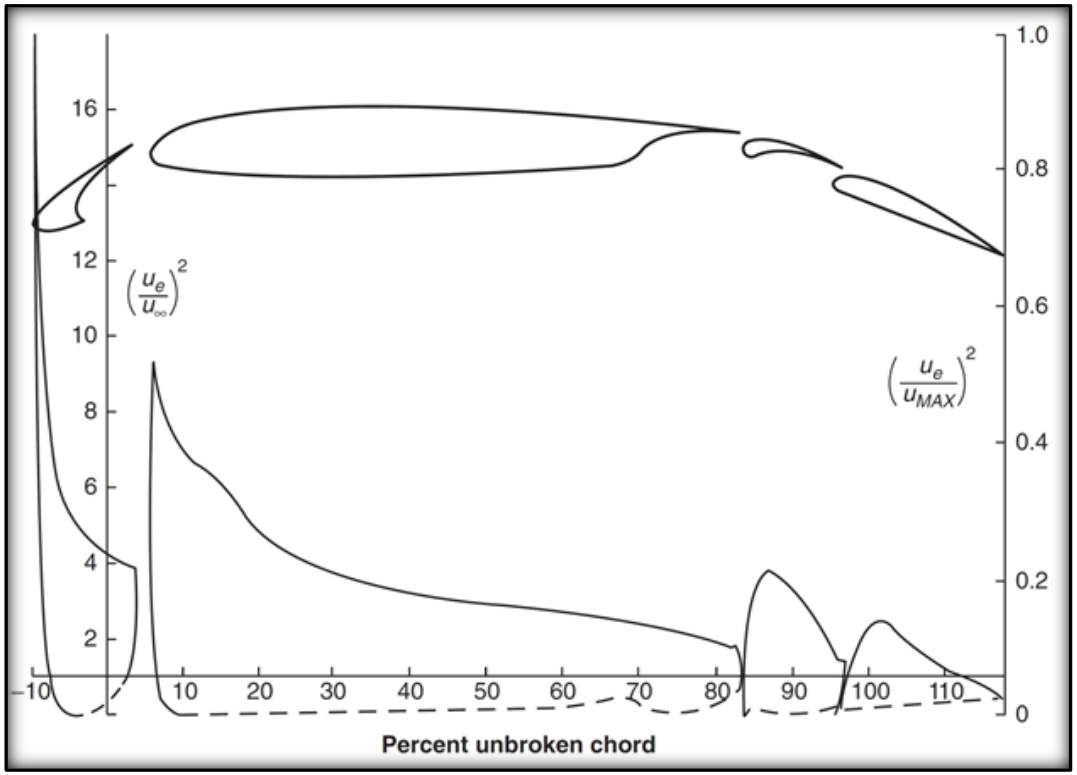

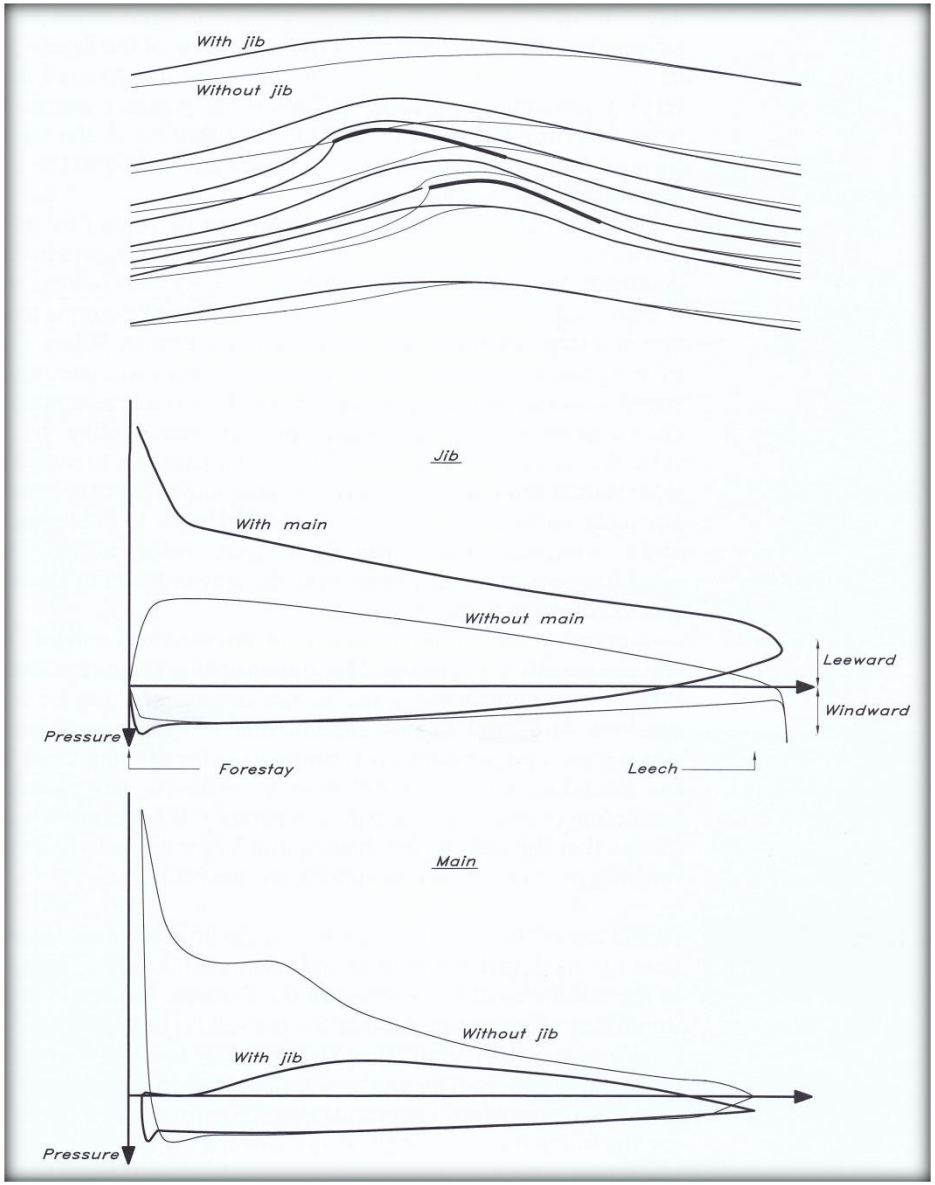

Interaction in multi-airfoil systems: aircraft super-lift system (top) jib-mainsail system (right, taken from Larsson, Eliasson, Principles of Yacht Design, 3 ed., McGraw Hill, 2007). Note that in the latter case the jib is loaded more, and the mainsail is loaded less than when working alone!

Bluff body aerodynamics

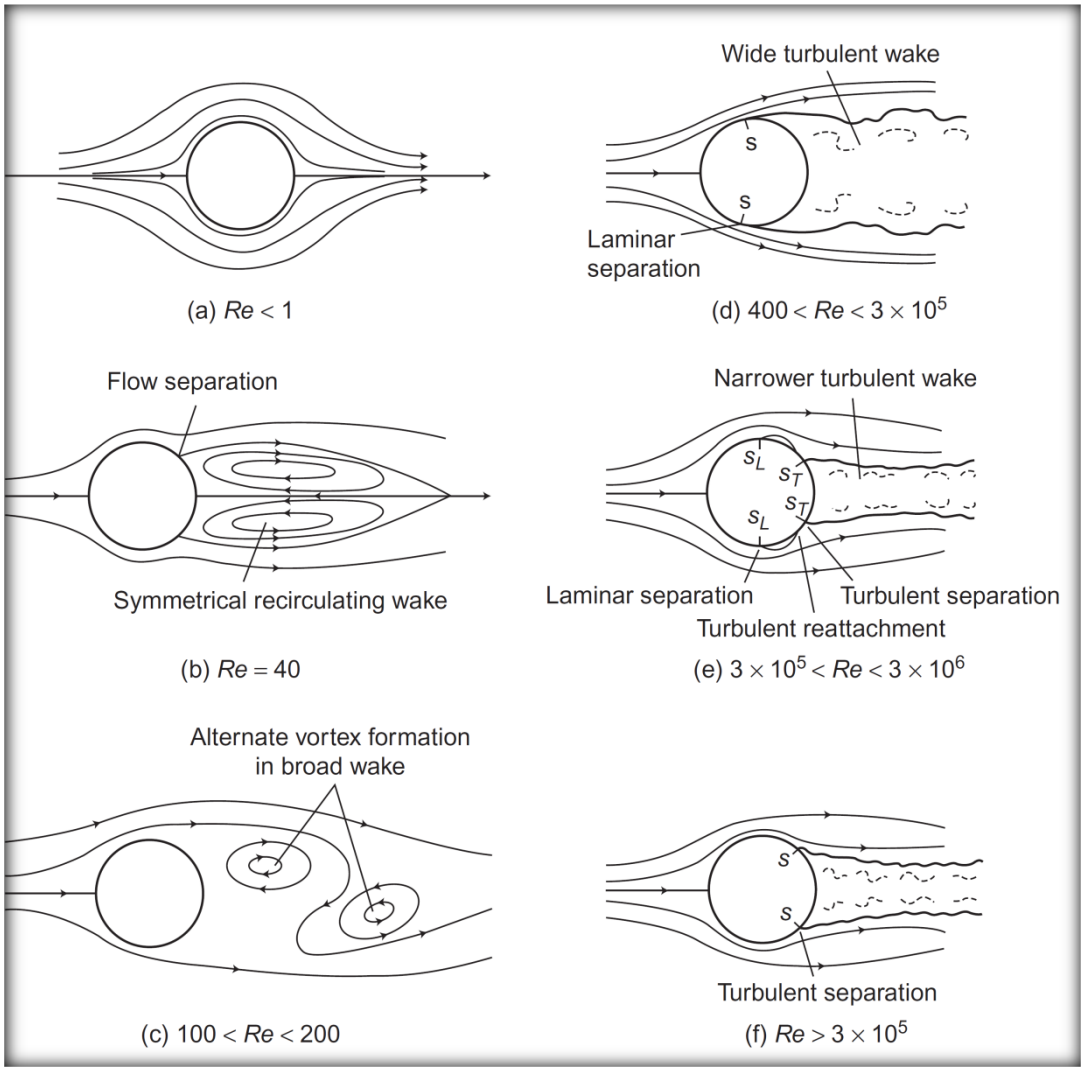

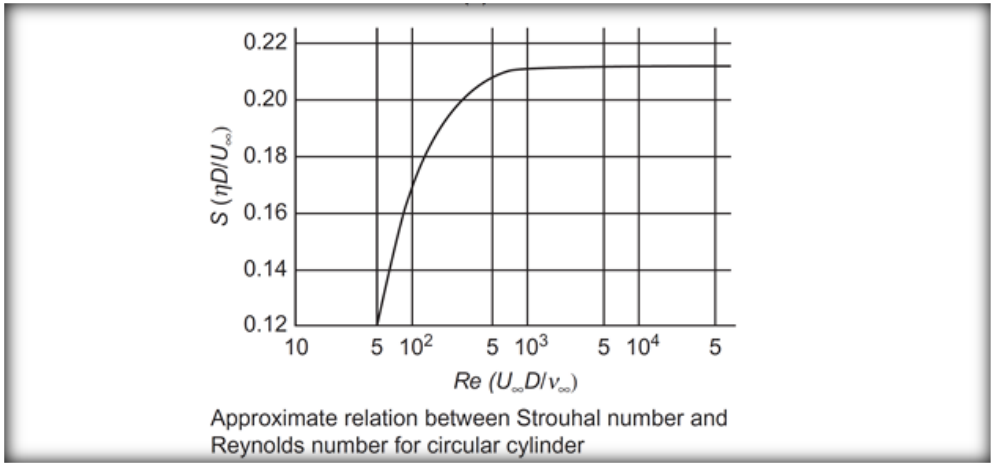

Approximate relation between Strouhal number and Reynolds number for circular cylinder

Left: different forms of a flow past a cylinder dependently on the Reynolds number.

Top: the Strouhal number of the main vortex structures in the wake behind the cylinder, plotted against the Reynolds number.

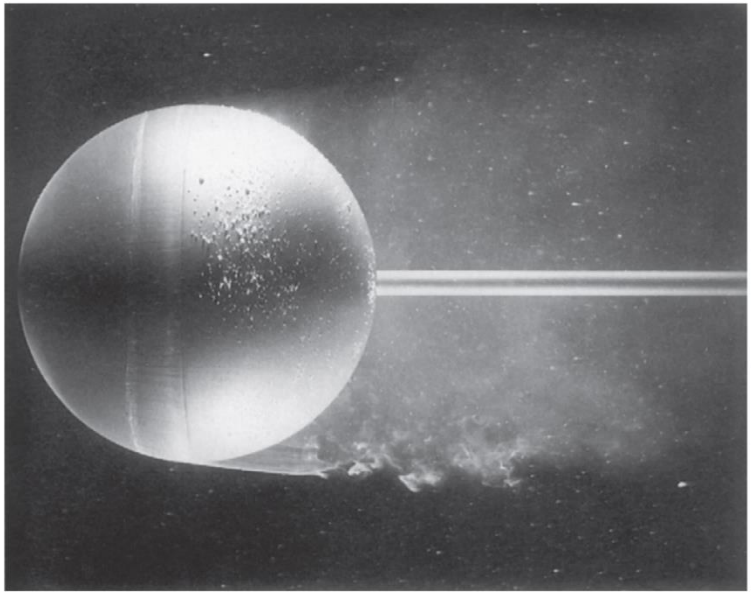

(a) $Re_D = 15{,}000$

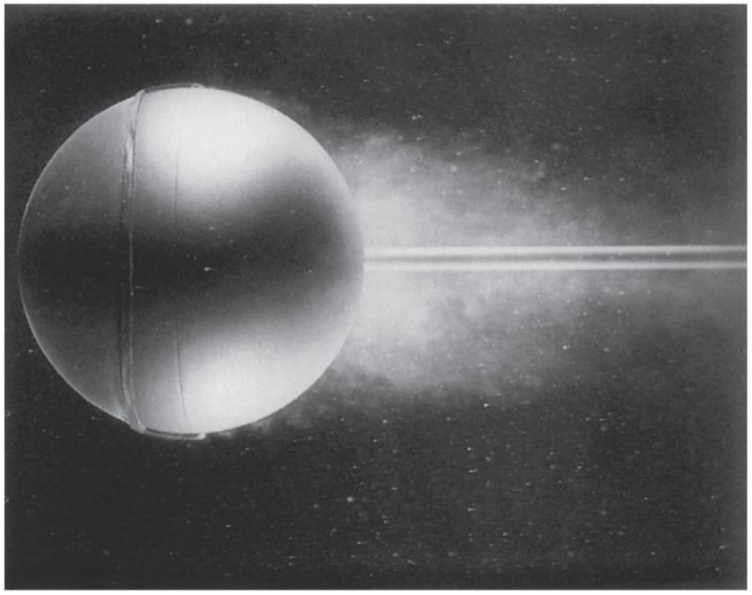

(b) $Re_D = 30{,}000$

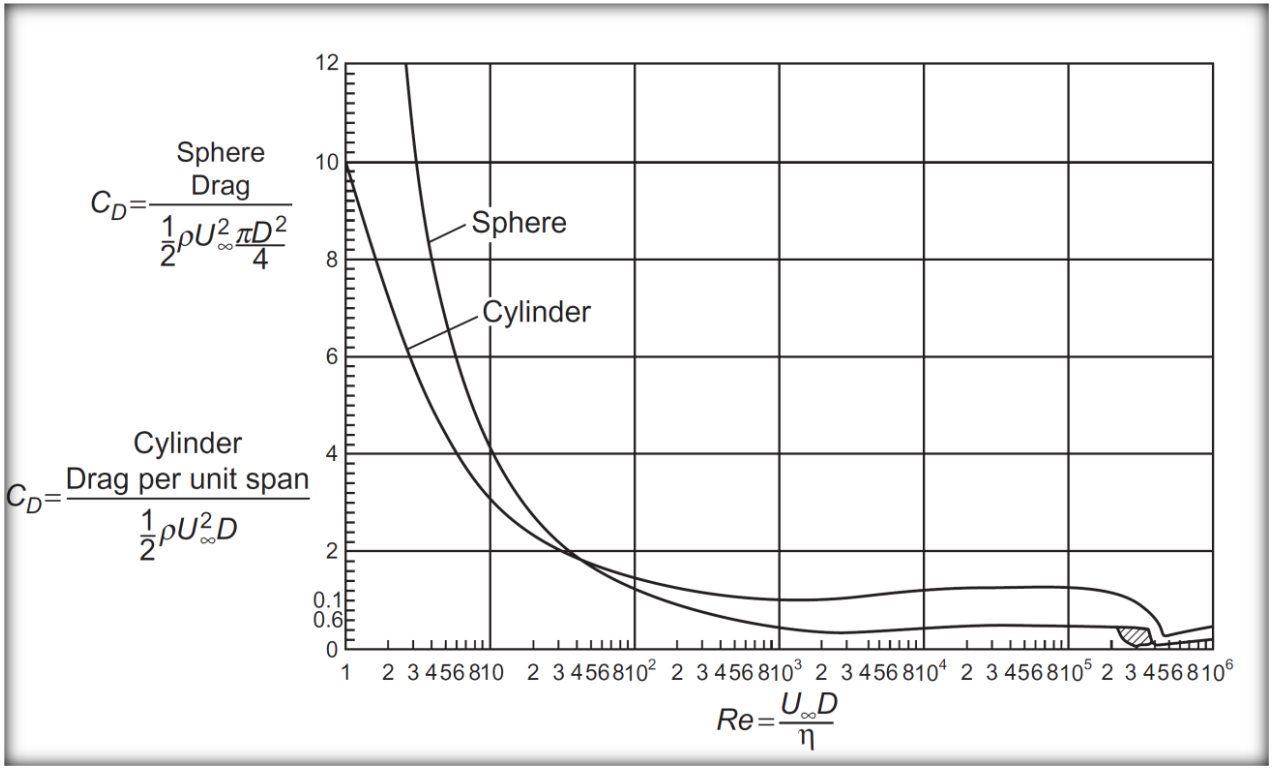

Top: Cylinder and sphere drag coefficients plotted against the Reynolds number.

Left: flow past a smooth sphere at Re=15000 (top) and the sphere with a tripping wire (forcing transition) at Re=30000 (bottom). Note that in the latter case the separation is delayed and the wake behind the sphere is much smaller. Also, drag is significantly reduced!